Neural Networks 142 (2021) 363–374

Contents lists available at ScienceDirect

Neural Networks

journal homepage: www.elsevier.com/locate/neunet

Classification of visuomotor tasks based on electroencephalographic data depends on age-related differences in brain activity patterns

C. Goelz [a], K. Mora [b,c], J. Rudisch [d], R. Gaidai [a], E. Reuter [e], B. Godde [f], C. Reinsberger [a], C. Voelcker-Rehage [d,g], S. Vieluf [a,h,*]

[a] Institute of Sports Medicine, Paderborn University, Paderborn, Germany
[b] Remote Sensing Centre for Earth System Research, Leipzig University, Leipzig, Germany
[c] German Centre for Integrative Biodiversity Research (iDiv), Leipzig, Germany
[d] Department of Neuromotor Behavior and Exercise, Institute of Sport and Exercise Sciences, University of Münster, Münster, Germany
[e] Department of Sport and Health Sciences, Technical University of Munich, Munich, Germany
[f] Department of Psychology & Methods, Jacobs University Bremen, Bremen, Germany
[g] Institute of Human Movement Science and Health, Chemnitz University of Technology, Chemnitz, Germany
[h] Division of Epilepsy and Clinical Neurophysiology, Department of Neurology, Boston Children's Hospital, Harvard Medical School, Boston, MA, USA

ARTICLE INFO

Article history:
Received 16 October 2020
Received in revised form 12 March 2021
Accepted 22 April 2021
Available online 13 May 2021

Keywords:
Dynamic mode decomposition
Fine motor control
Machine learning
Decoding
Dedifferentiation
Aging

ABSTRACT

Classification of physiological data provides a data driven approach to study central aspects of motor control, which changes with age. To implement such results in real-life applications for elderly it is important to identify age-specific characteristics of movement classification. We compared task-classification based on EEG derived activity patterns related to brain network characteristics between older and younger adults performing force tracking with two task characteristics (sinusoidal; constant) with the right or left hand. We extracted brain network patterns with dynamic mode decomposition (DMD) and classified the tasks on an individual level using linear discriminant analysis (LDA). Next, we compared the models' performance between the groups. Studying brain activity patterns, we identified signatures of altered motor network function reflecting dedifferentiated and compensational brain activation in older adults. We found that the classification performance of the body side was lower in older adults. However, classification performance with respect to task characteristics was better in older adults. This may indicate a higher susceptibility of brain network mechanisms to task difficulty in elderly. Signatures of dedifferentiation and compensation refer to an age-related reorganization of functional brain networks, which suggests that classification of visuomotor tracking tasks is influenced by age-specific characteristics of brain activity patterns. In addition to insights into central aspects of fine motor control, the results presented here are relevant in application-oriented areas such as brain computer interfaces.

1. Introduction

Decoding and classification of motor behavior based on EEG are elementary parts of EEG analysis and an essential basis for areas of application including, for example, brain computer interfaces (BCI) for persons with motor disabilities. BCI systems, designed to recognize movement specific brain states, require the identification of segregated functional brain networks and processes (Kasahara, DaSalla, Honda, & Hanakawa, 2015; Saha & Baumert, 2020). Considering the clinical application areas of BCIs, for example, in the field of stroke rehabilitation (Ramos-Murguialday et al., 2013) or in prevention and training, e.g., in form of neurofeedback (Gomez-Pilar, Corralejo, Luis, Alvarez, & Hornero, 2016), older adults form a main target group. More generally, the development of brain networks is an important factor which influences classification performance (Ahn & Jun, 2015). Although inter- and intrasubject variability are studied in recent research in the field of BCIs (Sannelli, Vidaurre, Müller, & Blankertz, 2019), the influence of age-related changes on classification results has been rarely investigated (Ahn & Jun, 2015). Chen, Fu, Boger, and Jiang (2019) found a 15.9% lower accuracy of the classification of body side when the left- and the right-hand were passively stimulated in older adults compared to younger adults. The authors suspect an association with altered, less lateralized, spatial patterns of EEG signals in the elderly compared to younger participants. Beyond that, the authors highlight the relevance of this finding, as lateralization of brain activity patterns based on the contralateral organization of the motor system

* Correspondence to: Paderborn University, Institute of Sports Medicine, Warburger Str. 100, 33098 Paderborn, Germany.
E-mail address: vieluf@sportmed.upb.de (S. Vieluf).

https://doi.org/10.1016/j.neunet.2021.04.029
0893-6080/

is often exploited in BCI algorithms. However, less is known about whether the results can be confirmed for active motor tasks that could allow a transfer to stroke rehabilitation for example. Furthermore, it has not yet been investigated whether the described changes also apply to other task dimensions. A thorough understanding of this would be a prerequisite for real-life applications.

In addition to the practical relevance of investigating the influence of age-related changes on the classification performance, the underlying machine learning models offer the possibility of a data-driven insight into the aging brain (Cichy & Pantazis, 2017; Schirrmeister et al., 2017). With increasing age, brain activity is less differentiated and noisier (Reuter-Lorenz & Lustig, 2005), i.e., brain networks are less task specific (Carp, Park, Hebrank, Park, & Polk, 2011). This is summarized under the term dedifferenciation (Reuter-Lorenz & Lustig, 2005). Therefore, it is reasonable to assume that decoding of neural signals might be less effective in older adults (Roland et al., 2011). Age-related changes include a reduction of distinctness and segregation in the functional organization of large-scale brain networks (Cassady, Ruitenberg, Reuter-Lorenz, Tommerdahl, & Seidler, 2020; Sala-Llonch, Bartrés-Faz, & Junqué, 2015). Using fMRI Seidler et al. (2010) showed functional brain activation to be more widespread and bilateral during visual and cognitive tasks. Several authors report similar results during motor tasks where older compared to younger participants showed stronger activation of the ipsilateral motor cortex (Carp et al., 2011; Ward & Frackowiak, 2003) as well as higher connectivity within sensorimotor and visual networks during visuomotor tapping (Cassady et al., 2020). Moreover, older adults seem to recruit additional sensory as well as prefrontal areas during motor tasks which has been interpreted as compensational mechanisms and additional recruitment of cognitive resources (Berghuis et al., 2019; Reuter-Lorenz & Cappell, 2008). Compensation hence implies that older adults use different neural circuits than young adults when performing a motor task (Cabeza, Anderson, Locantore, & McIntosh, 2002; Davis, Dennis, Daselaar, Fleck, & Cabeza, 2008; Heuninckx, Wenderoth, Debaere, Peeters, & Swinnen, 2005).

These changes are noticeable in altered spatial patterns and spectral composition of EEG signals (Al Zoubi et al., 2018) and thus influence the requirements for discriminability of task-relevant brain network processes for classification, as previously shown by Chen et al. (2019) for one task dimension, i.e., body side of execution. Expanding on these findings, the differentiability of electrophysiological brain network patterns of different task dimensions could provide insight into age-related alterations described above.

One possibility to study these patterns is offered by dynamic mode decomposition (DMD). This method, which originated in the field of fluid dynamics, is capable of detecting spatio-temporal coherent patterns from high dimensional data and has recently been applied in several neuroscientific settings (Brunton, Johnson, Ojemann, & Kutz, 2016; Gölz et al., 2018; Vieluf et al., 2018). DMD provides a framework to deduce brain activity patterns that relate to brain network characteristics, i.e., coherent dynamics of distinct sources (Fries, 2005). It allows to assess the pattern dynamics in terms of neuronal oscillations as markers of neuronal network dynamics by constructing a best fit linear dynamical system directly from the measurement data (Brunton et al., 2016). In a previous study, we were able to show age-related differences in EEG derived central control processes during a force maintenance task utilizing DMD (Vieluf et al., 2018). More specifically, we found that in older adults compared to younger adults' brain activity was less differentiated between left- and right-hand tasks. Furthermore, we could detect signs of a less segregated sensorimotor network, higher internal network communication as well as additional cognitive recruitment during force control in older adults.

To better understand these alterations and draw conclusions about their relevance in practical settings, we aimed to study the classification of fine motor movements in four visuomotor tracking tasks based on EEG recordings recorded in a follow-up experiment of Vieluf et al. (2018). First, by comparing electrophysiological differences between younger and older adults in relation to different tasks, we aimed to confirm previously reported age-related differences in EEG activity associated with visuomotor tasks. We expected that older adults have less differentiated and segregated networks, similar to our previous findings (Vieluf et al., 2018). Second, we investigated classification differences between age-groups. We expected to gain insight into the age-related differences in functional brain activity, such as higher bilateral brain activation, compensatory involvement and additional attentional resources by studying the discriminative performance in relation to the different task dimensions. Our findings provide further insights into age-related alterations of movement-related brain networks and show the practical relevance these alterations might have.

2. Methods

2.1. Participants

Twenty-six participants were included in this study. All participants enrolled voluntarily and gave their informed consent after recruitment through flyers, telephone calls, and newspaper announcements within the Bremen-Hand-Study@Jacobs (Voelcker-Rehage, Reuter, Vieluf, & Godde, 2013). A questionnaire was used to collect information about the demographic background and health status of all participants. All subjects described themselves as healthy and free of neurological diseases and had normal or corrected to normal hearing and vision. The Edinburgh Handedness Inventory (Oldfield, 1971) further identified all participants as right-handed. Participants received a compensation of 8 Euros per hour. The study was in accordance with the Declaration of Helsinki and approved by the ethics committee of the German Psychological Society. Based on their age, participants were assigned to a young adults (YA: N = 13, age = 18–25 years, 8 females, 5 males) or an older adults (OA: N = 13, age = 55–65 years, 8 females, 5 males) group.

2.2. Experimental procedure

Within the framework of the Bremen-Hand-Study@Jacobs (Voelcker-Rehage et al., 2013), participants took part in several experiments. The visuomotor force-control experiment analyzed here was designed as a force tracking experiment conducted blockwise. Participants sat about 80 cm in front of a computer screen (19", frame rate 60 Hz). Their arms rested on arm pads. Thumb and index finger grasped a force transducer (model Mini-40, ATI Industrial Automation, Garner, NC, United States) in a pinch grip. Using the right- or left-hand, the task was to follow a target force level for five seconds by applying the required amount of force to the force transducer. The target line was either presented as a constant level (steady), i.e., a straight line, corresponding to 2 N or as a sinusoidal curve (sine) ranging from 2 N to 12 N with a frequency of 1 Hz on the *y*-axis whereas time was presented on the *x*-axis. The time axis (x-axis) covered 5 s, allowing participants to see one second of the upcoming target line and 4 s of the preceding target line and the applied force. A total of 160 trials were carried out, each lasting 5 s with an individual break of 5 s to 7 s during which participants were instructed to focus on a fixation cross on the screen in front of

them. Initially, 80 trials were performed with the right hand. The first 40 trials involved the steady force level and the following 40 trials the sine force level. The sequence was then repeated with the left hand. The participants had an individual break between each task block. Prior to the experiment, the maximum voluntary contraction (MVC) was recorded with three maximum precision grip trials. Each grip lasted 5 s with approximately 2 min break in between.

The experiment and grip force acquisition were realized using customized LabVIEW (National Instruments, Austin) software. Grip force was recorded with 120 Hz sampling rate and amplitude resolution of 0.06 N via the force transducer.

EEG was recorded with 32 active electrodes (ActiveTwo, BioSemi, Amsterdam, Netherlands) placed on the scalp according to the international 10–20 System. Ocular artifacts as well as mastoid potential were recorded with additionally placed electrodes. Common Mode Sense (CMS) and Driven Right Leg (DRL) electrodes were placed next to Cz. All EEG signals were recorded with a sampling rate of 2048 Hz applying an online filter between 0.16 and 100 Hz. Prior to the experiments resting EEGs with eyes open and eyes closed were recorded for 30 s each while participants sat comfortably on a chair.

2.3. Data analysis

Data analysis was conducted using Python (version 3.7.6). For EEG data analysis and classification the additional MNE package (version 0.2.3 Gramfort et al., 2013) and scikit-learn (version 0.22.1, Pedregosa et al., 2011) were used. All data was analyzed on an individual level and the classifiers were trained individually for each participant. The procedure for individual EEG classification is outlined in Fig. 1 and described in detail in the following subsections.

2.3.1. Force data

Force data was analyzed to identify incorrect task execution using the central 3 s of each trial. The force signal was filtered using a 4th order Butterworth filter at 30 Hz. To evaluate the performance of each participant and test for correct task execution, we calculated the mean absolute deviation from the target force as an indicator of accuracy. Trials were excluded if their z-score was above three. Results are available in the supplementary material (Figure S1).

2.3.2. EEG data

EEG data was resampled to 200 Hz and re-referenced to the linked mastoids. Signals were bandpass filtered between 4 and 30 Hz using a FIR zero phase filter created with MNE python. To correct ocular artifacts caused by blinking and eye movements we applied ICA with the FastICA algorithm (Hyvärinen & Oja, 1997). When the source signals of a component correlated with the ocular signals, this component was automatically marked and set to zero before back projection. Next data was cut between 1 s and 4 s so that the middle 3 s of each trial were used for the analysis. Trials containing artifacts such as electrical or myogenetic artifacts were removed based on the *Autoreject* pipeline (Jas, Engemann, Bekhti, Raimondo, & Gramfort, 2017).

2.3.2.1. Dynamic mode decomposition. Each artifact free trial was mean centered and windows of 0.5 s (100 datapoints) were decomposed with DMD. Consecutive windows have an overlap of 0.25 s (50 datapoints) to account for data non-stationarities. The exact DMD algorithm proposed by Tu, Rowley, Luchtenburg, Brunton, and Kutz (2014) and used by Brunton et al. (2016) was applied in this work.

Basically, DMD is an algorithm that allows to approximate the relation of all signals in pairs of consecutive time instances of a measurement $X \in \mathbb{R}^{n\times m}$, where n denotes sensors and m denotes measurement points at time t. With DMD it is possible to decompose X to extract spatio-temporal patterns of coherent brain activation (Brunton et al., 2016). To increase the number of calculated DMD modes and thus improve the approximation accuracy we used the delay embedding technique as applied by Brunton et al. (2016); stacking depth $h = 4$ was selected. Since the DMD algorithm takes advantage of the Singular Value Decomposition (SVD), the optimal rank r of the input matrix and therefor the number of SVD modes was determined using the method of Donoho and Gavish (2014). The decomposed spatial patterns are organized in a matrix $\Phi \in \mathbb{C}^{hn\times r}$, containing all DMD modes (i.e., spatial patterns) and a diagonal matrix $\Lambda \in \mathbb{C}^{r\times r}$, containing the corresponding DMD eigenvalues. From this, the original measurement X can be approximated by the model:

$$\hat{X} = \Phi \exp(\Omega t) z,$$

where Ω contains the continuous eigenvalues transformed with

$$\Omega = \log(\Lambda)/\Delta t.$$

The variable t denotes time whereby $\Delta t = 0.005\ s$ and z is computed from the first data point x_1 of X with $x_1 = \Phi z$. From Ω we calculated the frequencies in cycles per second (Hz)

$$f = |\mathrm{imag}(\Omega)/2\pi|$$

for all DMD modes.

The optimal stacking depth h as well as window size and overlap were determined by an error analysis of the data of five randomly selected subjects. As unique spatial information is present in the first n rows of a mode, we used $\Phi \in \mathbb{C}^{n\times r}$.

2.3.2.2. Feature extraction. For feature extraction we modified and applied an approach based on Filter Bank Common Spatial Pattern (FBCSP; Ang, Chin, Wang, Guan, & Zhang, 2012). FBCSP is a widely used and very successful algorithm for classifying motion-related EEG signals. In essence, linear combinations of EEG channels are used to calculate weightings (spatial filters) that maximize the class discriminative energy for selected frequency bands. The spatial filters in each frequency band of interest are usually calculated based on the Common Spatial Pattern (CSP) algorithm. The rationale behind this was to extract the information from the DMD modes of all windows that would allow the best possible differentiation between the tasks. In this way it is possible to relate the results of the classification to differences in brain network activity.

To estimate spatial filters, we first extracted the absolute DMD values associated with the θ-(4 to $<$ 7 Hz), α-(7 to $<$ 12 Hz), β_1-(12 to $<$ 16 Hz) and β_2-(16 to $<$ 30 Hz) frequencies creating a mode matrix Φ_b for each frequency band b. For each frequency band we extracted the spatial filters from the training data with the CSP algorithm. More precisely, we calculated the transformation matrix $W_b \in \mathbb{R}^{n\times n}$ by solving the generalized eigenvalue problem:

$$S_{b,1} W_b = (S_{b,1} + S_{b,2}) W_b D_b.$$

$S_{b,1}$ and $S_{b,2}$ represent estimates of the covariance matrices of the b-th mode matrix Φ_b of the respective task and D_b contains the eigenvalues of $S_{b,1}$ on its diagonal (Ang et al., 2012). Each column vector w_{bj} is called spatial filter. For each frequency band we extracted the two most informative spatial filters w_{bj}, i.e., columns of W_b forming the transformation matrix $\overline{W}_b$ as described in Barachant, Bonnet, Congedo, and Jutten (2010). This number was chosen to avoid overfitting and is based on preliminary tests that showed no significant improvement in classifier performance when more filters were selected. The MNE Python implementation of the CSP algorithm modified for our purposes was used here. Multiclass CSP is implemented from Grosse-Wentrup and Buss (2008).

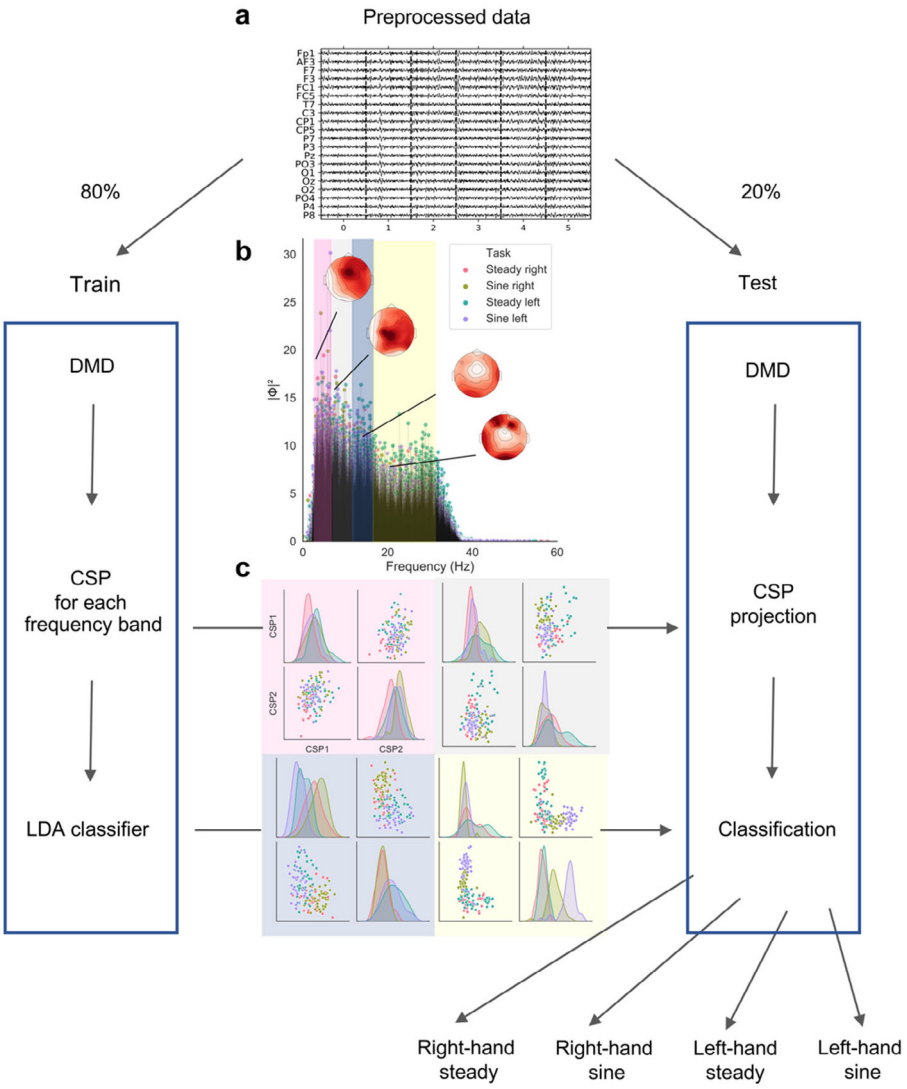

Fig. 1. Individual classification approach. For each participant preprocessed data epochs (a) are divided in training and test data set. Each set was next decomposed by DMD (b: DMD spectrum and corresponding spatial pattern). DMD mode magnitudes corresponding to the θ, α, β_1 or β_2 frequency bands were spatially filtered and projected into CSP Space (c). A LDA classifier was trained on the training data and applied to the test data set.

2.3.2.3. Classification. After preprocessing, all trials were assigned to either a training or test data set. The ratio of this allocation comprised 80% training (i.e., 32 trials per class) and 20% test (i.e., 8 trials per class). Subsequently, all trials were segmented in overlapping windows and decomposed using DMD as described above. For task classification a Linear Discriminative Analysis (LDA) classifier with shrinkage was trained and tested for each participant using the scikit-learn toolbox implemented in Python (Pedregosa et al., 2011). As features the DMD mode magnitudes in each frequency band b and trial i, $\Phi_{b,i}$, were projected into CSP space with the transformation matrix $\overline{W}_b$, which was extracted from the training data. Next, the logarithmic variance of the projected DMD mode magnitudes of all time windows was calculated and used as features as described in Barachant et al. (2010). Thus, for each trial and frequency band the CSP feature $v_{b,i}$ was calculated with

$$v_{b,i} = \log(\mathrm{Var}(\overline{W}_b^T \Phi_{b,i})),$$

using training and test data, respectively. The CSP features $v_{b,i}$ are then collected in the matrix $V \in \mathbb{R}^{t \times 2f}$ where t denotes the total number of trials and f the total number of frequency bands used (see Fig. 1 for a visual presentation of the procedure). Note that $2f$ is required to reflect the frequency bands from both training and test data. To (1) chose the best hyperparameter of the LDA classifier (solver, number of components) and to (2) determine the metrics of the classifier, 10 × 10 fold cross-validation was applied. More precisely the procedure was run in two loops. In the outer loop, the data set was split into training and test data. In a second inner loop, the best hyperparameters of the classification algorithm were determined using 10-fold cross-validation. This procedure was repeated 10 times. In each fold, the classification performance was evaluated based on accuracy, F1 value, and receiver operating characteristics curve (ROC). Accuracy indicates the absolute percentage of all correctly classified trials, whereas the F1 value is the weighted average of the precision and recall. To evaluate the classifier performance in terms of discriminative ability we further studied the ROC (see Fig. 6) and used the area under the curve as metric (ROC AUC). As ROC is restricted to binary classification problems, we relied on the one vs. all procedure implemented in scikit-learn to calculate the ROC AUC for the 4-class classification, thus restricted Fig. 6 to the two-class cases.

Classification was carried out at different levels. First, a four-class classification was carried out. All trials of the four different tasks were included. Then, two-class classifications were

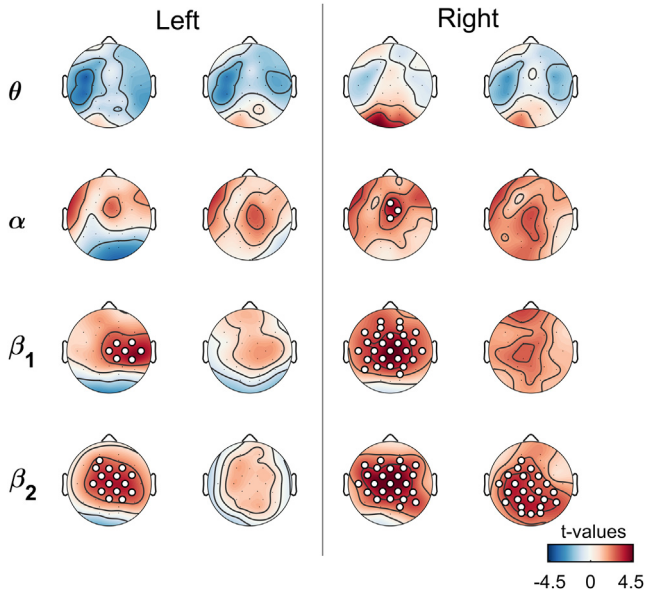

Fig. 2. Comparison of DMD mean mode magnitude between groups in left- and right-hand sine and steady tasks displayed as statistical t-maps (red: OA > YA, blue: OA < YA). Significant differences are marked with white circles (FDR corrected p-value < 0.05). (For interpretation of the references to color in this figure legend, the reader is referred to the web version of this article.)

performed to compare the classifier performance for each task dimension separately. With this approach we intended to study all levels of classification and intend to increase comparability to two-class approaches reported in the literature (Chen et al., 2019). First all left- and right-handed trials were classified as one class regardless of whether it was a sine or steady tracking task. Next, all sine or steady-tracking trials, regardless of whether the trial was performed with the left- or right-hand, were used as one class each. In order to ensure the comparability of this classification step, we selected 20 trials of each class randomly in each fold. Thus, 40 trials each were the basis for the left- and right-hand as well as sine and steady task classifications. Lastly, the classification was performed for the following combinations: left-hand sine vs. left-hand steady, right-hand sine vs. right-hand steady, left-hand sine vs. right-hand sine, left-hand steady vs. right-hand steady.

2.4. Statistics

Statistical Analysis was conducted using SPSS for MAC version 24.0 (IBM Corp., Armonk, NY, USA) and MNE Python (version 0.2.3 Gramfort et al., 2013). Following Brunton et al. (2016) and Vieluf et al. (2018) the DMD mean mode magnitudes were calculated per frequency band and task for statistical comparison. For this, DMD modes of all windows and trials associated with the θ-(4 to < 7 Hz), α-(7 to < 12 Hz), β_1-(12 to < 16 Hz) and β_2-(16 to < 30 Hz) frequencies per task and per participant obtaining DMD mean mode magnitudes per task per frequency band for each participant. To describe the input feature basis prior to CSP feature extraction and LDA classification we compared the DMD mean mode magnitudes between groups and between tasks. We used permutation t-tests to account for the high dimensionality of the EEG data and therefore the inaccuracies in test assumption requirements and reduction of type I and type II errors (Maris & Oostenveld, 2007). P-values were corrected with false discovery rate (Benjamini & Hochberg, 1995). To test for group differences in laterality we calculated the difference between C3 and C4. Moreover, to test for additional frontal activation we calculated the difference between Pz and Fz. Values below 0 indicate higher DMD mean mode magnitudes on the central right or frontal electrode, respectively. Values above 0 indicate higher DMD mean mode magnitudes on the central left or parietal side. We analyzed these indices each with repeated measures analysis of variance (ANOVA) with the between factor group (2; YA and OA) and the within factor task (4; right-hand steady, right-hand sine, left-hand steady, left-hand sine) for each frequency band (θ, α, β_1, β_2). Significant interactions and main effects were followed by Bonferroni corrected pairwise comparisons. In case of violation of the assumption of sphericity we use the Greenhouse–Geisser correction and report corrected degrees of freedom and p-values. The effect sizes are reported as η_p^2.

We compared the classifier performance measures (accuracy, ROC AUC and F1) between groups with Mann–Whitney U test due to violations of normality assumption. Effect sizes are reported as r-values. All statistical tests were conducted on significance level set to $\alpha = 0.05$.

3. Results

3.1. Group and task comparison of DMD mean modes

The group comparisons of DMD mean mode magnitudes are illustrated in Fig. 2 as topographic t-maps. Significant differences, obtained with permutation t-tests, are marked as white circles ($p < 0.05$). For a better understanding of the classifier input and to maintain a direct link to the classification, here we report absolute DMD patterns (note that this procedure is different than in Vieluf et al., 2018 where task related DMD values are reported). For the left-hand steady tasks, we found significant differences between the groups on central electrodes in the β_1 and the β_2 frequency band, with higher DMD mean mode magnitudes for the OA group. Group comparison of the right-hand tasks revealed significant higher DMD mean mode magnitudes in the α, β_1 and β_2 band over central, frontal and parietal electrodes for the steady task. Significant group differences for the right-hand sine task were observed for central, parietal, and occipital electrodes in the β_2 range.

Comparisons of left- and right-hand sine as well as left- and right-hand steady tasks are illustrated in Fig. 2 as topographic t-maps for the OA and YA groups separately. Comparing left- and right-hand tasks, we found significant task differences over occipital electrodes in the θ-band for the steady task in the OA group. In the YA group, significant differences between the left and right-hand sine tasks were evident over central, parietal and occipital electrodes in the β bands localized on the left side. Regarding the comparison of sine and steady tasks we found differences in occipital electrodes which were present for the right-hand task in the YA group and in the left-hand task in the OA group (all $p < 0.05$).

Comparing C3C4 indices with repeated measures ANOVA revealed a significant interaction between task and group in the β_1 band [$F(1.96, 47.193) = 3.214$, $p = 0.05$, $\eta_p^2 = 0.118$] and the β_2 band [$F(2.42, 58.166) = 3.22$, $p = 0.038$, $\eta_p^2 = 0.118$]. Post-hoc comparison revealed significant differences between YA and OA in the left-hand steady task for the β_1 frequency band with lower values for OA. In the β_2 range in the right-hand sine task, the OA showed higher values (all $p < 0.05$; see Fig. 4a).

For PzFz indices the task-by-group interaction was significant for the α band [$F(1.75, 42.11) = 8.34$, $p = 0.001$, $\eta_p^2 = 0.258$]. Post-hoc tests revealed a significant difference between the groups in the left-hand steady task ($p = 0.005$) with higher values for the YA.

In the θ and β_1 bands there was a significant main effect of task for the PzFz indices [θ: $F(3, 72) = 6.06$, $p = 0.001$, $\eta_p^2 =$

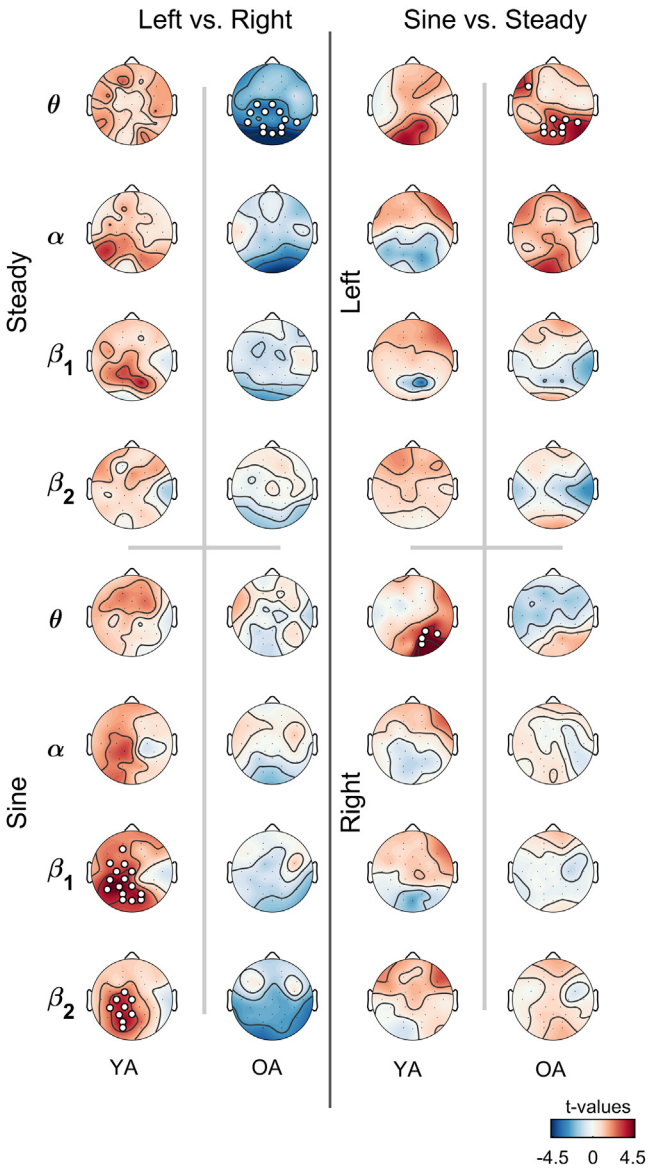

Fig. 3. Comparisons of DMD mean mode magnitudes between left- and right-hand as well as sine and steady tasks within groups displayed as statistical t-maps. Significant differences are marked with white circles (FDR corrected p-value $<$ 0.05). Red: Right $>$ Left/Steady $>$ Sine, Blue: Right $<$ Left/Steady $<$ Sine. (For interpretation of the references to color in this figure legend, the reader is referred to the web version of this article.)

0.394; β_1: F(3, 72) = 9.156, p = 0.006, $\eta_p^2 = 0.447$], but no main effect of group [θ: F(1, 24) = 0.55, p = 0.47, $\eta_p^2 = 0.018$; β_1: F(1, 24) = 0.159, p = 0.694, $\eta_p^2 = 0.007$]. Pairwise comparisons revealed significant differences between the right-hand steady, right-hand sine and left-hand sine tasks in the θ band with lower values in the left-hand steady task. In the β_1 band participants had higher values in the left-hand steady task compared to both hands sine tasks and lower values in the left-hand sine compared to the right-hand sine task (all p $<$ 0.05; see Fig. 4b).

In summary, we found group differences of spatio-temporal coherent patterns in all tasks involving central electrodes. By comparing the tasks, these patterns revealed higher task specificity. This was indicated by fewer significant differences, especially between the sine tasks which were more pronounced in the YA. In addition, we found selective differences between OA and YA of the coherent patterns with regard to laterality and frontality.

3.2. Evaluation of classifier performance

All classifiers performed significantly above chance level for both groups (p $<$ 0.05). Regarding the group comparison, the four-class classification revealed no significant difference between groups in all performance metrics (accuracy: U = 54.5, p = 0.125, r = 0.30; F1: U = 57.00, p = 0.169, r = 0.28; ROC AUC: U: 57.00, p = 0.169, r = 0.28). However, visualizing the classifiers performance in an error or a confusion matrix (Fig. 5), on a descriptive level, classification accuracy was higher in the group of YA for the dimension body side (9.75 % wrongly classified compared to 18 % in the OA group). Conversely, accuracy seemed to be reduced in the group of YA for the dimension task characteristic (14.25 % wrongly classified compared to 10.5 % in the OA group, see confusion matrix Fig. 5).

Following this observation, we compared the classifier performance of left-hand vs. right-hand and sine vs. steady task classification separately. Furthermore, to check whether the differences are differently expressed between the body side and task characteristics levels we considered all the binary classifications as a follow up analysis. The performance of all two-class classifiers at both levels is shown as ROC curves in Fig. 6. All classification results are shown in Tables 1 and 2 for each participant. Mann–Whitney U test confirmed significantly higher accuracy, F1 and ROC AUC scores for the left-hand vs. right-hand classification in the YA compared to the OA group (accuracy: U = 39.5, p = 0.019, r = 0.45; F1: U = 40.00, p = 0.022, r = 0.45; ROC AUC: U = 43.00, p = 0.034, r = 0.42). For the sine vs. steady classification Mann–Whitney U test confirmed significantly lower accuracy, F1 and ROC AUC scores for the YA compared to the OA group (accuracy: U = 40.00, p = 0.022, r = 0.45; F1: U = 41.00, p = 0.026, r = 0.44; ROC AUC: U = 37.00, p = 0.014, r = 0.48) (see Fig. 6a and b top panel ROC curves).

Next, we compared the classification of each task. There were significant differences between the groups only for the left-hand sine vs. right-hand sine task with higher scores in the YA group (left-hand vs. right-hand sine: accuracy: U = 29.00, p = 0.003, r = 0.56; F1: U = 29.00, p = 0.003, r = 0.56; ROC AUC: U = 41.00, p = 0.026, r = 0.44; left-hand vs. right-hand steady: accuracy: U = 69.00, p = 0.448, r = 0.15; F1: U = 71.00, p = 0.511, r = 0.14; ROC AUC: U = 71.00, p = 0.511, r = 0.14). The follow up analysis of the individual comparisons sine vs. steady revealed no significant difference between the groups for the right- and left-hand sine vs. steady classification separately (left-hand sine vs steady: accuracy: U = 59.5, p = 0.204, r = 0.25; F1: U = 59.00, p = 0.204, r = 0.26; ROC AUC: U = 53.00, p = 0.113, r = 0.32; right-hand sine vs steady: accuracy: U = 57.00, p = 0.169, r = 0.28; F1: U = 57.00, p = 0.169, r = 0.28; ROC AUC: U = 52.00, p = 0.101, r = 0.33) (see Fig. 6c).

In essence, the four-class classification showed comparable performance in both groups. However, the investigation of false positive and negative rates revealed differences between age groups. These could be confirmed by examining the binary classification. While the classification of the body side performed better in YA, the classification of task characteristics was better in OA.

4. Discussion

In the current study, we aimed to explore differences in spatio-temporal coherent patterns related to brain network characteristics relevant for the classification of visuomotor tracking tasks based on EEG recordings between YA and OA. Following up on

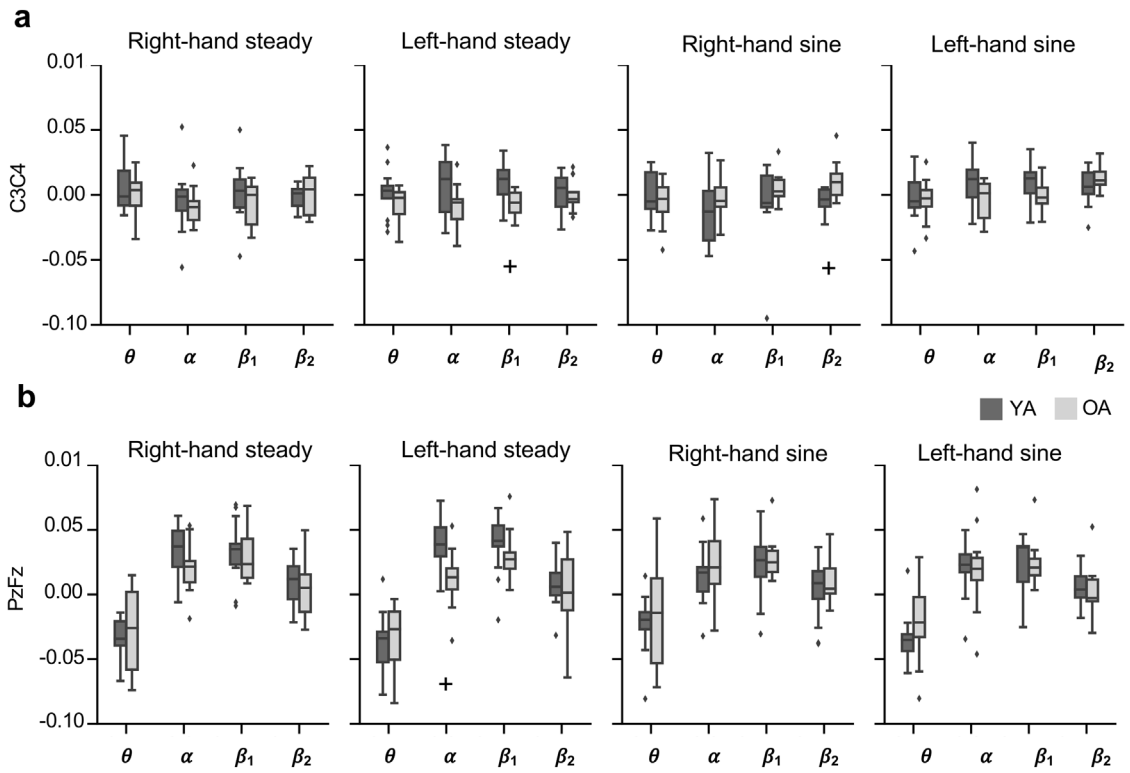

Fig. 4. Laterality and frontality indices calculated based on the DMD mean mode magnitudes. C3C4 indices (a) and PzFz (b) indices for each frequency band and task. Significant differences between the groups are marked with +.

Table 1
First level: Classification performance of 10 × 10 fold cross validation.

	4 class			sine vs. steady			left vs. right		
	Accuracy	ROC AUC	F1	Accuracy	ROC AUC	F1	Accuracy	ROC AUC	F1
OA1	0.85	0.97	0.84	1.00	1.00	1.00	0.80	0.88	0.80
OA2	0.59	0.85	0.58	0.87	0.95	0.87	0.69	0.80	0.68
OA3	0.65	0.85	0.65	0.83	0.90	0.83	0.68	0.80	0.66
OA4	0.55	0.78	0.55	0.71	0.78	0.70	0.75	0.83	0.75
OA5	0.71	0.92	0.71	0.89	0.96	0.89	0.74	0.85	0.73
OA6	0.47	0.74	0.46	0.71	0.76	0.70	0.74	0.81	0.73
OA7	0.72	0.92	0.72	0.88	0.96	0.87	0.73	0.79	0.72
OA8	0.63	0.86	0.63	0.79	0.86	0.79	0.72	0.77	0.71
OA9	0.53	0.76	0.52	0.79	0.87	0.78	0.63	0.67	0.63
OA10	0.65	0.86	0.64	0.91	0.97	0.91	0.63	0.72	0.61
OA11	0.76	0.92	0.75	0.88	0.93	0.87	0.75	0.84	0.73
OA12	0.48	0.74	0.47	0.89	0.96	0.89	0.57	0.58	0.56
OA13	0.64	0.87	0.63	0.97	1.00	0.97	0.69	0.77	0.68
YA1	0.57	0.84	0.56	0.69	0.78	0.68	0.90	0.95	0.90
YA2	0.73	0.90	0.72	0.66	0.73	0.66	0.91	0.96	0.91
YA3	0.71	0.89	0.70	0.71	0.78	0.71	0.68	0.75	0.67
YA4	0.67	0.89	0.66	0.75	0.82	0.75	0.91	0.98	0.91
YA5	0.78	0.94	0.77	0.66	0.75	0.66	0.95	0.98	0.95
YA6	0.85	0.97	0.84	0.87	0.94	0.87	0.99	1.00	0.99
YA7	0.76	0.93	0.76	0.83	0.93	0.83	0.77	0.88	0.77
YA8	0.54	0.79	0.53	0.61	0.69	0.61	0.70	0.76	0.69
YA9	0.56	0.78	0.54	0.79	0.82	0.79	0.59	0.58	0.58
YA10	0.63	0.83	0.62	0.60	0.69	0.59	0.64	0.70	0.62
YA11	0.73	0.94	0.73	0.77	0.84	0.76	0.93	0.97	0.92
YA12	0.69	0.90	0.68	0.91	0.94	0.91	0.87	0.92	0.87
YA13	0.82	0.94	0.82	0.94	0.98	0.94	0.83	0.90	0.83

Vieluf et al. (2018), we studied differences in the extracted patterns between groups in four visuomotor tracking task (sine and steady force tracking executed with the left and right hand) to get insights into which brain activity patterns might influence the classification.

Group differences in all tasks were most pronounced for central electrodes, especially in the β_2 band. Between groups, we found task differences when comparing left- and right-hand sine tasks in frontal and central electrodes in the θ and α bands. Assuming additional bilateral and frontal recruitment for older adults we calculated central laterality (C3C4) and fronto-parietal indices (PzFz) and found significant group differences. Especially the central laterality index as well as the gradient between frontal and parietal of the left-hand steady tasks in the α band was lower in OA. Moreover, we found differences in the central laterality index of the right-hand sine task in β_2. Taken together, these

Table 2
Second level: Classification performance of 10 × 10 fold cross validation.

	sine: left vs. right			steady: left vs. right			left: sine vs. steady			right: sine vs. steady		
	Accuracy	ROC AUC	F1	Accuracy	ROC AUC	F1	Accuracy	ROC AUC	F1	Accuracy	ROC AUC	F1
OA1	0.85	0.93	0.85	0.96	1.00	0.96	1.00	1.00	1.00	1.00	1.00	1.00
OA2	0.81	0.90	0.81	0.96	0.99	0.96	0.93	0.99	0.93	0.99	1.00	0.99
OA3	0.74	0.86	0.73	0.81	0.89	0.81	0.93	0.97	0.92	0.78	0.87	0.77
OA4	0.76	0.85	0.76	0.81	0.89	0.81	0.81	0.93	0.80	0.79	0.88	0.79
OA5	0.63	0.63	0.62	0.94	0.99	0.93	0.91	0.97	0.91	0.91	0.99	0.91
OA6	0.76	0.85	0.76	0.74	0.81	0.73	0.70	0.79	0.69	0.81	0.91	0.81
OA7	0.85	0.94	0.85	0.83	0.92	0.82	0.94	0.99	0.94	1.00	1.00	1.00
OA8	0.91	0.99	0.91	0.91	0.98	0.91	0.95	0.99	0.95	0.93	0.97	0.93
OA9	0.63	0.67	0.63	0.89	0.95	0.89	0.88	0.95	0.87	0.83	0.92	0.82
OA10	0.74	0.85	0.73	0.76	0.81	0.75	0.99	1.00	0.99	0.84	0.91	0.84
OA11	0.85	0.89	0.84	0.92	0.97	0.92	0.90	0.95	0.90	0.89	0.97	0.88
OA12	0.79	0.90	0.78	0.68	0.78	0.67	0.93	0.98	0.92	0.89	0.97	0.89
OA13	0.79	0.87	0.79	0.89	0.96	0.89	0.94	0.99	0.94	0.99	1.00	0.99
YA1	0.92	0.96	0.92	0.87	0.96	0.87	0.84	0.92	0.84	0.82	0.93	0.82
YA2	0.96	0.99	0.96	0.93	0.96	0.92	0.68	0.79	0.67	0.83	0.93	0.82
YA3	0.90	0.95	0.90	0.96	1.00	0.96	0.71	0.77	0.71	0.90	0.97	0.90
YA4	0.98	0.99	0.97	0.92	0.96	0.92	0.91	0.96	0.91	0.81	0.87	0.81
YA5	0.97	1.00	0.97	0.93	0.98	0.93	0.86	0.94	0.85	0.72	0.85	0.72
YA6	0.99	1.00	0.99	1.00	1.00	1.00	0.86	0.95	0.86	0.98	1.00	0.97
YA7	0.91	0.98	0.91	0.88	0.96	0.87	0.98	1.00	0.98	0.96	0.98	0.96
YA8	0.77	0.82	0.76	0.82	0.91	0.82	0.71	0.77	0.71	0.74	0.78	0.74
YA9	0.75	0.83	0.75	0.76	0.80	0.75	0.85	0.93	0.85	0.70	0.71	0.69
YA10	0.68	0.73	0.67	0.79	0.89	0.79	0.96	1.00	0.96	0.71	0.77	0.70
YA11	0.99	1.00	0.99	0.94	0.98	0.94	0.77	0.85	0.77	0.90	0.97	0.90
YA12	0.86	0.90	0.85	0.88	0.91	0.87	0.97	0.98	0.97	0.89	0.95	0.89
YA13	0.97	0.99	0.97	0.86	0.93	0.85	0.96	1.00	0.96	0.96	1.00	0.96

differences could be indicative of altered motor network function reflecting dedifferentiated and compensational brain activation. This could be a decrease in the segregation of the network as well as the need for integration of different central control processes related to attentional processes.

Classification accuracies were above chance level for each of the four visuomotor tracking tasks. Focusing on the two dimensions, task characteristics (sine vs. steady) and body side (left-hand vs right-hand), showed that the performance of the left vs. right-hand task classification was better in YA, and the classification performance of the sine vs. steady task was better in the OA independent of the body side of execution. This reduced body side specificity with age might be a result of a reduction in segregation of the motor network seen e.g., in lateralization of brain activation in OA as described above. Furthermore, our findings indicate that classification of tasks based on their characteristics is more accurate for OA, which might relate to a reorganization of central processes with age.

4.1. Group and task comparison of DMD mean modes

In the following section we first discuss DMD-derived brain activity patterns (related to analysis depicted in Figs. 2–4), which formed the basis of the task classification. For a better understanding of the classification results and their relation to neurophysiological changes, it is helpful to consider the input characteristics. We did not correct for a baseline to ensure a stronger relationship between DMD results and the classifier performance. Therefore, these results must be considered in light of age-related differences that are already evident in resting networks (Sala-Llonch et al., 2015).

In our previous paper, we reported less segregated sensorimotor network activation and higher need of information integration in OA reflected in higher β_2 activation (Vieluf et al., 2018). Extending those findings, we can confirm higher β DMD mean mode magnitudes, i.e., higher energy of spatially correlated structures in the group of OA consistently in all tasks at (fronto- and parieto-) central electrodes as shown in Fig. 2. Differences in the more complex sine task additionally included occipital electrodes in the β_2 band that were restricted to the right-hand task. Such changed functional connectivity of central (motor) areas with frontal, parietal, and occipital areas might point to altered motor network functioning in OA (Hong, Liu, Sun, & Tong, 2016; Seidler et al., 2010). The β band has been discussed in terms of the integration and exchange of information in different networks (Hipp, Engel, & Siegel, 2011). Thus, the β band specific differences could indicate a greater need of the integration of attention- and sensory-related information processing in the group of OA as proposed by Vieluf et al. (2018). Albeit speculatively, these differences may reflect higher demands in maintaining status quo of the sensorimotor system due to higher level of noise and dedifferentiated activation of the motor system as reported with aging (Reuter-Lorenz & Lustig, 2005). Besides, it should be noted that for the least complex steady right-task, we found higher α DMD modes in OA over frontal electrodes. The α band has been associated with attentional processes (Klimesch, 2012). More specifically, increased α power in cognitive as well as visuomotor tasks have been suggested to reflect an increased engagement of visual spatial attention (Baravalle, Guisande, Granado, Rosso, & Montani, 2019; Van Diepen, Foxe, & Mazaheri, 2019). Thereby α power gates the attentional focus, by suppressing the processing of irrelevant stimuli, locations, or features (Jensen & Mazaheri, 2010). Thus, increased frontal α DMD mode magnitudes even in the relatively easiest task might indicate an increased need to engage attentional control processes for OA.

To investigate the hypothesis of less differentiation in brain activity in OA, we compared groupwise DMD mean mode magnitudes between the tasks (see Fig. 3). DMD mean mode magnitudes differed most prominently between the right- and left-hand tasks. This was stronger in the group of YA and most prominent in the sine tracking task which could point to different motor control strategies (Siegel, Donner, & Engel, 2012; Yordanova, Falkenstein, & Kolev, 2020) as well as different motor representation of the left- and right-hand task as found in fMRI (Carp et al., 2011) and EEG (Pfurtscheller, 2001) investigations.

Based on reports on the activation of bilateral motor areas in unimanual tasks with age (Carp et al., 2011; Ward & Frackowiak, 2003) we calculated laterality indices of sensorimotor relevant

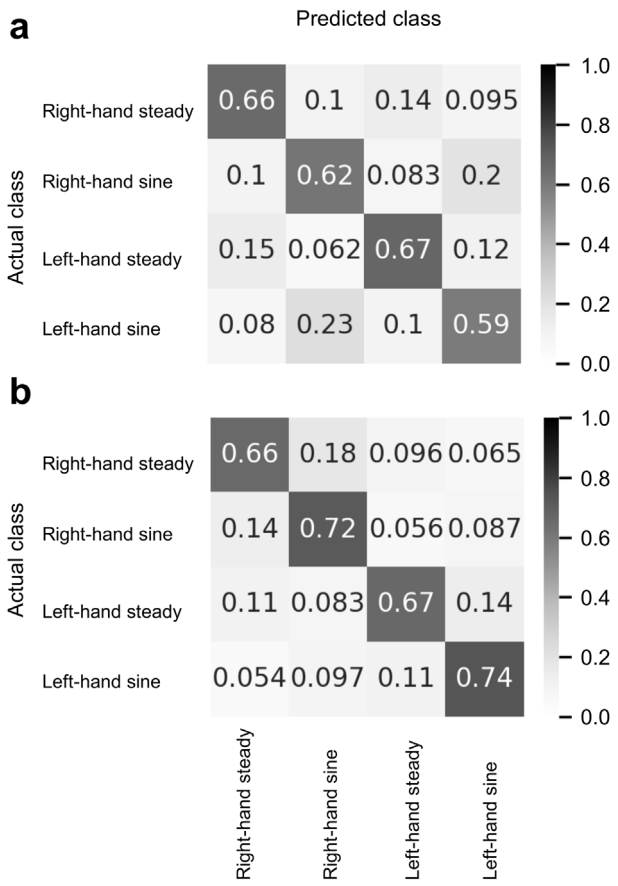

Fig. 5. Confusion Matrix of the 4-class classification. OA (a) and the YA group (b).

electrodes (C3 and C4; see Fig. 4a). We found higher, i.e., more positive lateralization indices, in the β_1 frequency band for the left-hand steady task and lower, i.e., more negative lateralization indices, for the right-hand sine task comparing YA to OA. Such differences in lateralization could point to higher ipsilateral DMD mean mode magnitudes and might correspond to the higher relevance of bilateral recruitment with age, which has been previously interpreted as compensatory involvement and dedifferentiated activation (i.e., less contralateral organization) of neural resources of the motor system (Carp et al., 2011; Sailer, Dichgans, & Gerloff, 2000; Zich, Debener, De Vos, Frerichs, Maurer, & Kranczioch, 2015). With the current results, we cannot clearly differentiate between both effects due to the high complexity and interrelation of these effects as well as the high heterogeneity of the behavioral results in the OA (see Figure S1, supplementary material). This is also reflected in the lack of clear correlations between the behavioral level and the laterality and frontality indices. Thus, both effects could be present in the group. Future work designed to dissociate between these alternatives might, however, test this in different performance groups and with more high-resolution methods. Nevertheless, we found no correlations between the laterality indices and behavioral performance, which could indicate a rather independent non-compensatory effect (see supplementary material Figure S3).

We further expected to find signs of recruitment of brain areas related to attentional processes as described in Vieluf et al. (2018) and calculated frontality indices between Fz and Pz (see Fig. 4b). We assumed this to be reflected in higher frontal activation in older adults especially present in the θ frequency band (Reuter-Lorenz & Cappell, 2008). However, frontality indices in the θ range did not differ between age groups. Nevertheless, there is a group difference in the α band in the left-hand steady task with values closer to zero indicative of a lower gradient between frontal and parietal α activity in OA. As described above, this could be an expression of altered attentional control (Klimesch, 2012). We assume that changes in attentional and additional cognitive recruitment could be shown more clearly on the basis of task-related analyses.

4.2. Classification performance

In the following, we focus on the results of the classification (summarized in Figs. 5 and 6). We will discuss these findings in relation to above-described age-related brain networks alterations. The classification of the tasks achieved accuracies above chance level in both groups. Nevertheless, we found differences in the classification of the task dimensions (body side: left-hand vs. right-hand and task characteristic: sine vs. steady) between the groups as shown in Fig. 6. Regarding the classification of the body side, the classifier achieved lower performance scores in the OA group, only in the more complex task (sine tracking task). This is in line with Chen et al. (2019) as well as Zich et al. (2015). Chen et al. (2019) found reduced accuracies in the classification of body side of a passive stimulation task in older adults. Zich et al. (2015) compared overt and covert movements and found lower body side classification accuracies for older adults. Both author groups relate their findings to a reduced laterality of sensorimotor rhythms in older adults. Similarly, we found age-related changes in laterality, but only in the left-hand steady task as well as the right-hand sine task. Besides, DMD mean mode magnitudes of left- and right-hand sine tasks differed significantly only in the group of YA. This body side specific differences confirms task specificity, which could be due to higher lateralization of brain activation as indication of classification performance. We assume lower distinctiveness of the motor system in older adults (Carp et al., 2011; Cassady et al., 2020; Ward & Frackowiak, 2003). Moreover, the poorer classification performance of the left-hand and right-hand tasks could be explained by this finding. Interestingly, we did not find a lower classifier performance in OA compared to YA in the left-hand vs. right-hand steady tasks. This might suggest that the age-related loss of segregation is more pronounced in more complex tasks. This finding could further indicate a dependence of task complexity for dedifferentiated brain activation as reported for the motor system in older adults (Carp et al., 2011) and extends these previous findings. Taken together the classification results could be an indicator of general reorganization processes and related to aforementioned DMD differences found in this study as well as in Vieluf et al. (2018).

Whereas Chen et al. (2019) and Zich et al. (2015) only report differences in classification performance by body side, we extend these findings by including differences in the classification of task characteristics (sine vs. steady). Similar to above mentioned lower distinctiveness of the motor system in OA, we expected a lower classifier performance in the OA. However, we found a higher classification performance in the group of OA independent of the side of task execution. This finding may indicate that different task demands may have caused rather more diverse brain activity patterns in OA than in YA. Looking at the group differences of the DMD mean modes, it seems that the age-related differences in the less complex tasks are more pronounced, while the groups in the more complex tasks show more similar brain activity patterns. As discussed above, this may be due to a greater need for integration of attentional and sensory information for OA particularly evident in the less complex task, which may be reflected in the differences in the frontality index. However, in OA such integration could be highly depended on the task characteristic as indicated by the classifier results.

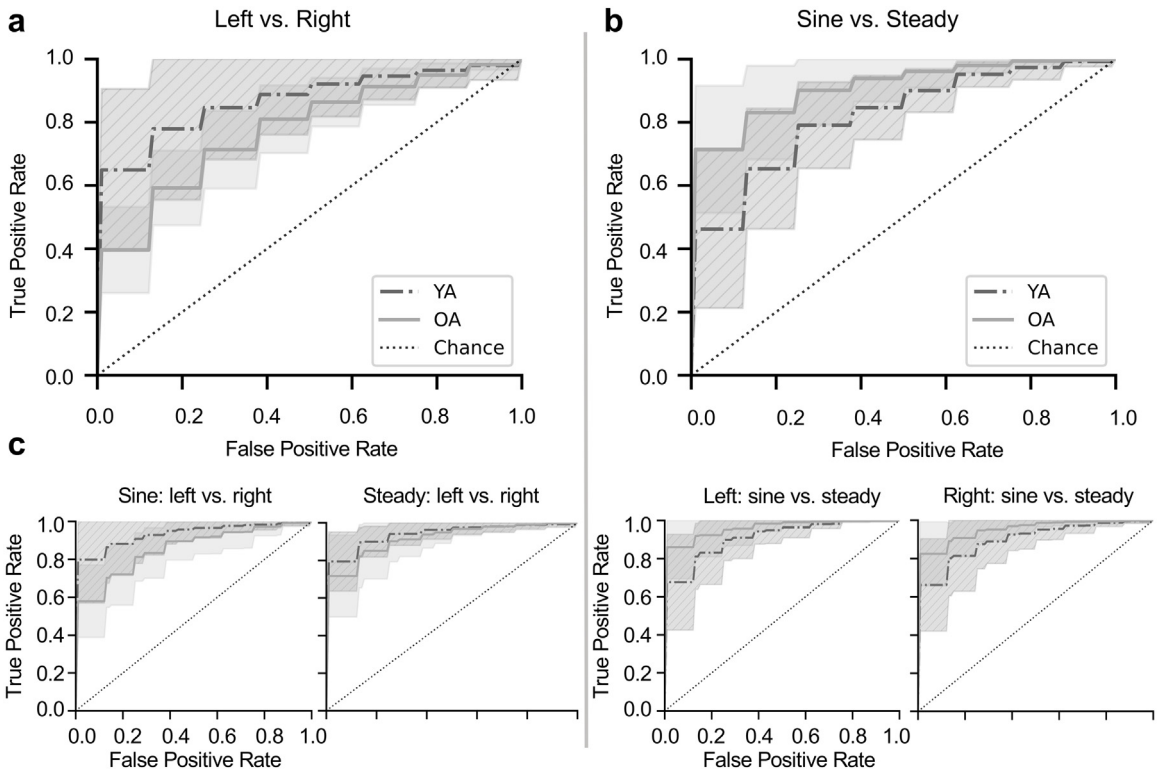

Fig. 6. ROC curve of both two-class classifiers as stepwise classification approach. ROC curves represent the group mean with associated standard deviation as gray (OA) and gray striped (YA) areas. a: left vs. right; b: sine vs. steady; c: sine: left vs. right, steady: left vs. right, left: sine vs. steady, and right: sine vs. steady (from left to right).

In sum, we confirmed previously reported differences in classification performance between tasks (Chen et al., 2019) now for fine motor control tasks and show for the first time the relationship between classification and task characteristics in older adults. We extended the existing knowledge and detect classification results, which depend on processes relevant to attention. Not only the laterality but also the activation of attention-related processes, could be an important factor for classification performance. This observation is supported by BCI systems relying on attention relevant processes like systems based on the P300 shape and dynamics as well as systems based on steady state evoked potentials/response (SSVEP/R) (Abiri, Borhani, Sellers, Jiang, & Zhao, 2019; Middendorf, McMillan, Calhoun, & Jones, 2000). Although they are not rooted in the exploitation of sensorimotor signals used here, they indicate the relevance of attentional processes.

Considering age-related changes in electrophysiological brain activity patterns detected with DMD as well as the classification results, we were able to show indications of the reorganization of central mechanisms in fine-motor force control tasks. Besides the practical relevance, it was also possible to capture age-related changes on the basis of the classifier performance. Machine learning algorithms and multivariate methods such as DMD can thus contribute to data-driven research on age-related changes and extend classical EEG analyses without making assumptions of the underlying data.

Our findings suggest that the influence of individual neurophysiological properties should be integrated into the development of BCI systems, as suggested by Blankertz et al. (2010). In addition, target group-specific characteristics, such as age-related differences, should be incorporated into the design process of BCI systems. This could include the use of age-specific electrode placement and the selection of suitable features and algorithms.

4.3. Methodological consideration

The data collection of the current study was embedded in a larger study context in which participants performed active fine motor control and sensory perception tasks. As a consequence, task classification was done based on an active task rather than on covert movements or passive stimulation as reported in the literature (Chen et al., 2019; Zich et al., 2015). This bears several advantages, first of all, by using an active task we could demonstrate the feasibility of classification in young and older adults. Second, by monitoring the motor outcome, we could account for noncompliance. Non-compliance is seen as one of the reasons for low classification performance in motor imaginary BCI systems (Blankertz et al., 2010). Third, having active tasks facilitated the classification of task characteristic and thus extending previous findings of age-related differences on classification performance (Chen et al., 2019; Zich et al., 2015). Therefore, however, the transferability of our results to BCI settings based on motor imaginary might be limited.

Furthermore, the block design of the trials as well as the broader context of the Bremen-Hand-Study@Jacobs might have impacted the results. In the context of the overall study frame, similar fine motor tracking tasks were repeatedly performed. On one hand, this had the advantage that we can assume that the participants were already familiar with the experimental procedure. On the other hand, plastic changes or training effects that have already taken place could mask age-related effects and might have influenced the classification performance. In contrast, we believe that intensive practice could have been beneficial for the interpretability of the data, as it eliminated age-specific differences in short-term adjustment effects. Finally, regarding the age of the participants, it is important to note that the group of OA was comparatively young (55–65 years old), so that even older participants might show more pronounced changes.

Another aspect to consider is using an alternative machine learning approach. Of course, other approaches might result in different classification performances and could account at least partly for neurophysiological changes as described in Blankertz et al. (2010) for example, with adaptive classification and neural networks. In particular, deep learning methods can automatically learn unexplored features, which could also yield high accuracy for both YA and OA. However, these methods are more suitable for large amounts of data which we do not currently have and often act as a "black box". This study uses an LDA classifier. The choice of this method, as well as the selection of the chosen parameters could have had an influence on the results. To determine the optimal parameters individually, we used an approach called hyperparameter tuning with Grid Search implemented in Scikit-learn (Pedregosa et al., 2011). Furthermore, we compared the results of the LDA classification with other common algorithms (Random Forest, Support Vector Machine) and obtained comparable results (see Supplementary Material Tables S1 and S2). Moreover, we chose the FBCSP algorithm, on which we based our approach, in combination with an LDA classifier, a very commonly used and in several BCI competitions benchmarked algorithm (Schirrmeister et al., 2017). To extract the features, we have used DMD to create the filter banks preliminary to the CSP. The patterns extracted via DMD based on the interrelation of the EEG signals can be related to the characteristic coherent behavior of physiological networks. Thus, this approach differs from the graph analytical approach of networks constructed by applying bivariate connectivity of EEG signals. DMD was recently found to be highly successful in classifying fine motor tasks (Shiraishi et al., 2020). Moreover, we successfully applied this method in previous work to extract age- and expertise-related sensorimotor network dynamics (Vieluf et al., 2018).

4.4. Conclusion

Based on age-related changes of brain networks, such as additional recruitment of bilateral motor areas (Carp et al., 2011; Ward & Frackowiak, 2003) and attentional resources (Berghuis et al., 2019), we aimed to study differences in the classification of EEG data recorded in active visuomotor tracking tasks.

In summary we found electrophysiological patterns associated with an altered sensorimotor network in OA. Lower task specificity in combination with changes in symmetry of brain activity point to bilateral and dedifferentiated, i.e., less task specific, brain activity of the motor network and activation and interrelation of several networks with age.

Most importantly these electrophysiological brain activity patterns resulted in lower classification performance in the classification of body side of task execution in OA, indicating less segregated brain network activation of the motor system. In contrast, OA showed higher classification performance with respect to the task characteristic. The study of the classifier input indicates the relevance of markers of information integration for classification performance in OA.

The current results confirm previous findings on age-related reorganization of task-related brain networks and expand them with reference to the characteristics of the task. Furthermore, the findings may have practical implications for areas of applied research such as BCI applications. Age-related differences should be taken into account in the development of BCI and neurofeedback systems if they are designed for this target group. This could include the selection of the appropriate positioning of electrodes, e.g., the use of frontal and occipital electrodes, as well as the choice of suitable features and algorithms.

Code availability

Python source code that supports the results is available from: https://github.com/christiangoelz/Code_Classification-of-visuomotor-tasks-YAOA

CRediT authorship contribution statement

C. Goelz: Analyzed data, design and implementation of the work including interpretation of the results, drafting parts of the work. **K. Mora:** Analyzed data, design and implementation of the work including interpretation of the results, drafting parts of the work. **J. Rudisch:** Design and implementation of the work including interpretation of the results, drafting parts of the work. **R. Gaidai:** Analyzed data, design and implementation of the work including interpretation of the results, drafting parts of the work. **E. Reuter:** Conceived and planned the experiments, design and implementation of the work including interpretation of the results, drafting parts of the work. **B. Godde:** Conceived and planned the experiments, design and implementation of the work including interpretation of the results, drafting parts of the work. **C. Reinsberger:** Design and implementation of the work including interpretation of the results, drafting parts of the work. **C. Voelcker-Rehage:** Conceived and planned the experiments, design and implementation of the work including interpretation of the results, drafting parts of the work. **S. Vieluf:** Conceived and planned the experiments, design and implementation of the work including interpretation of the results, drafting parts of the work.

Declaration of competing interest

The authors declare that they have no known competing financial interests or personal relationships that could have appeared to influence the work reported in this paper.

Acknowledgments

We thank Janine Ohmann and Sandra Fellehner for their support during data collection.

All authors approved the final version of the manuscript and agreed to be accountable for all aspects of the work.

Funding

The research was supported by the Deutsche Forschungsgemeinschaft (DFG, German Research Foundation, VO 1432/7-1 - SPP 1184 and DFG Project-ID 416228727 - SFB 1410). The study was supported within the framework of the equal opportunities concept 2 of the Paderborn University and by the Heinz Nixdorf Westfalian Foundation.

Appendix A. Supplementary data

Supplementary material related to this article can be found online at https://doi.org/10.1016/j.neunet.2021.04.029.

References

Abiri, R., Borhani, S., Sellers, E. W., Jiang, Y., & Zhao, X. (2019). A comprehensive review of EEG-based brain–computer interface paradigms. *Journal of Neural Engineering*, *16*(11001).

Ahn, M., & Jun, S. C. (2015). Performance variation in motor imagery brain–computer interface: A brief review. *Journal of Neuroscience Methods*, *243*, 103–110.

Al Zoubi, O., Ki Wong, C., Kuplicki, R. T., Yeh, H.-w., Mayeli, A., Refai, H., et al. (2018). Predicting age from brain EEG signals—A machine learning approach. *Frontiers in Aging Neuroscience*, *10*(184).

Ang, K. K., Chin, Z. Y., Wang, C., Guan, C., & Zhang, H. (2012). Filter bank common spatial pattern algorithm on BCI competition IV datasets 2a and 2b. *Frontiers in neuroscience*, *6*(39).

Barachant, A., Bonnet, S., Congedo, M., & Jutten, C. (2010). Common spatial pattern revisited by Riemannian geometry. In *2010 IEEE international workshop on multimedia signal processing* (pp. 472–476). IEEE.

Baravalle, R., Guisande, N., Granado, M., Rosso, O. A., & Montani, F. (2019). Characterization of visuomotor/imaginary movements in EEG: An information theory and complex network approach. *Frontiers in Physics*, *7*.

Benjamini, Y., & Hochberg, Y. (1995). Controlling the false discovery rate: a practical and powerful approach to multiple testing. *Journal of the Royal Statistical Society Series B-Methodological*, *57*, 289–300.

Berghuis, K. M. M., Fagioli, S., Maurits, N. M., Zijdewind, I., Marsman, J. B. C., Hortobágyi, T., et al. (2019). Age-related changes in brain deactivation but not in activation after motor learning. *NeuroImage*, *186*, 358–368.

Blankertz, B., Sannelli, C., Halder, S., Hammer, E. M., Kübler, A., Müller, K. R., et al. (2010). Neurophysiological predictor of SMR-based BCI performance. *NeuroImage*, *51*, 1303–1309.

Brunton, B. W., Johnson, L. A., Ojemann, J. G., & Kutz, J. N. (2016). Extracting spatial–temporal coherent patterns in large-scale neural recordings using dynamic mode decomposition. *Journal of Neuroscience Methods*, *258*, 1–15.

Cabeza, R., Anderson, N. D., Locantore, J. K., & McIntosh, A. R. (2002). Aging gracefully: compensatory brain activity in high-performing older adults. *Neuroimage*, *17*, 1394–1402.

Carp, J., Park, J., Hebrank, A., Park, D. C., & Polk, T. A. (2011). Age-related neural dedifferentiation in the motor system. *PloS One*, *6*(e29411-e29411).

Cassady, K., Ruitenberg, M., Reuter-Lorenz, P., Tommerdahl, M., & Seidler, R. (2020). Neural dedifferentiation across the lifespan in the motor and somatosensory systems. *Cerebral Cortex*, *30*, New York, N.Y.

Chen, M. L., Fu, D., Boger, J., & Jiang, N. (2019). Age-related changes in vibrotactile EEG response and its implications in BCI applications: A comparison between older and Younger populations. *IEEE Transactions on Neural Systems and Rehabilitation Engineering*, *27*, 603–610.

Cichy, R. M., & Pantazis, D. (2017). Multivariate pattern analysis of MEG and EEG: A comparison of representational structure in time and space. *NeuroImage*, *158*, 441–454.

Davis, S., Dennis, N., Daselaar, S., Fleck, M., & Cabeza, R. (2008). Que PASA? The posterior-anterior shift in aging. *Cerebral Cortex*, *18*(5), 1201–1209.

Donoho, D., & Gavish, M. (2014). The optimal hard threshold for singular values is. *IEEE Transactions on Information Theory*, *60*.

Fries, P. (2005). A mechanism for cognitive dynamics: neuronal communication through neuronal coherence. *Trends in Cognitive Sciences*, *9*, 474–480.

Gölz, C., Voelcker-Rehage, C., Mora, K., Reuter, E.-M., Godde, B., Dellnitz, M., et al. (2018). Improved neural control of movements manifests in expertise-related differences in force output and brain network dynamics. *Frontiers in Physiology*, *9*(1540).

Gomez-Pilar, J., Corralejo, R., Luis, L., Alvarez, D., & Hornero, R. (2016). Neurofeedback training with a motor imagery-based BCI: neurocognitive improvements and EEG changes in the elderly. *Medical & Biological Engineering & Computing*, *54*.

Gramfort, A., Luessi, M., Larson, E., Engemann, D., Strohmeier, D., Brodbeck, C., et al. (2013). MEG and EEG data analysis with MNE-Python. *Front. Neurosci.*, *7*, 267.

Grosse-Wentrup, M., & Buss, M. (2008). Multi-class common spatial patterns and information theoretic feature extraction. *IEEE Transactions on Bio-Medical Engineering*, *55*, 1991–2000.

Heuninckx, S., Wenderoth, N., Debaere, F., Peeters, R., & Swinnen, S. P. (2005). Neural basis of aging: the penetration of cognition into action control. *The Journal of Neuroscience*, *25*, 6787–6796.

Hipp, J. F., Engel, A. K., & Siegel, M. (2011). Oscillatory synchronization in large-scale cortical networks predicts perception. *Neuron*, *69*, 387–396.

Hong, X., Liu, Y., Sun, J., & Tong, S. (2016). Age-related differences in the modulation of small-world brain networks during a Go/NoGo task. *Frontiers in Aging Neuroscience*, *8*(100).

Hyvärinen, A., & Oja, E. (1997). A fast fixed-point algorithm for independent component analysis. *Neural Computation*, *9*, 1483–1492.

Jas, M., Engemann, D. A., Bekhti, Y., Raimondo, F., & Gramfort, A. (2017). Autoreject: Automated artifact rejection for MEG and EEG data. *Neuroimage*, *159*, 417–429.

Jensen, O., & Mazaheri, A. (2010). Shaping functional architecture by oscillatory alpha activity: Gating by inhibition. *Frontiers in Human Neuroscience*, *4*(186).

Kasahara, K., DaSalla, C. S., Honda, M., & Hanakawa, T. (2015). Neuroanatomical correlates of brain–computer interface performance. *NeuroImage*, *110*, 95–100.

Klimesch, W. (2012). Alpha-band oscillations, attention, and controlled access to stored information. *Trends in Cognitive Sciences*, *16*, 606–617.

Maris, E., & Oostenveld, R. (2007). Nonparametric statistical testing of EEG- and MEG-data. *Journal of Neuroscience Methods*, *164*, 177–190.

Middendorf, M., McMillan, G., Calhoun, G., & Jones, K. S. (2000). Brain-computer interfaces based on the steady-state visual-evoked response. *IEEE Transactions on Rehabilitation Engineering*, *8*, 211–214.

Oldfield, R. C. (1971). The assessment and analysis of handedness: the Edinburgh inventory. *Neuropsychologia*, *9*, 97–113.

Pedregosa, F., Varoquaux, G., Gramfort, A., Michel, V., Thirion, B., Grisel, O., et al. (2011). Scikit-learn: Machine learning in Python. *ThE Journal of Machine Learning Research*, *12*, 2825–2830.

Pfurtscheller, G. (2001). Functional brain imaging based on ERD/ERS. *Vision Research*, *41*, 1257–1260.

Ramos-Murguialday, A., Broetz, D., Rea, M., Läer, L., Yilmaz, Ö, Brasil, F. L., et al. (2013). Brain–machine interface in chronic stroke rehabilitation: A controlled study. *Annals of Neurology*, *74*, 100–108.

Reuter-Lorenz, P. A., & Cappell, K. A. (2008). Neurocognitive aging and the compensation hypothesis. *Current Directions in Psychological Science*, *17*, 177–182.

Reuter-Lorenz, P. A., & Lustig, C. (2005). Brain aging: reorganizing discoveries about the aging mind. *Current Opinion in Neurobiology*, *15*, 245–251.

Roland, J., Miller, K., Freudenburg, Z., Sharma, M., Smyth, M., Gaona, C., et al. (2011). The effect of age on human motor electrocorticographic signals and implications for brain–computer interface applications. *Journal of Neural Engineering*, *8*(46013).

Saha, S., & Baumert, M. (2020). Intra- and inter-subject variability in EEG-based sensorimotor brain computer interface: A review. *Frontiers in Computational Neuroscience*, *13*(87).

Sailer, A., Dichgans, J., & Gerloff, C. (2000). The influence of normal aging on the cortical processing of a simple motor task. *Neurology*, *55*, 979–985.

Sala-Llonch, R., Bartrés-Faz, D., & Junqué, C. (2015). Reorganization of brain networks in aging: a review of functional connectivity studies. *Frontiers in Psychology*, *6*(663).

Sannelli, C., Vidaurre, C., Müller, K. R., & Blankertz, B. (2019). A large scale screening study with a SMR-based BCI: Categorization of BCI users and differences in their SMR activity. *PLoS One*, *14*, Article e0207351.

Schirrmeister, R. T., Springenberg, J. T., Fiederer, L. D. J., Glasstetter, M., Eggensperger, K., Tangermann, M., et al. (2017). Deep learning with convolutional neural networks for EEG decoding and visualization. *Human Brain Mapping*, *38*, 5391–5420.

Seidler, R. D., Bernard, J. A., Burutolu, T. B., Fling, B. W., Gordon, M. T., Gwin, J. T., et al. (2010). Motor control and aging: Links to age-related brain structural, functional, and biochemical effects. *Neuroscience & Biobehavioral Reviews*, *34*, 721–733.

Shiraishi, Y., Kawahara, Y., Yamashita, O., Fukuma, R., Yamamoto, S., Saitoh, Y., et al. (2020). Neural decoding of electrocorticographic signals using dynamic mode decomposition. *Journal of Neural Engineering*, *17*.

Siegel, M., Donner, T., & Engel, A. (2012). Spectral fingerprints of large scale neuronal interactions. *Nature Reviews. Neuroscience*, *13*, 121–134.

Tu, J. H., Rowley, C. W., Luchtenburg, D. M., Brunton, S. L., & Kutz, J. N. (2014). On dynamic mode decomposition: Theory and applications. *Journal of Computational Dynamics*, *1*(391).

Van Diepen, R. M., Foxe, J. J., & Mazaheri, A. (2019). The functional role of alpha-band activity in attentional processing: the current zeitgeist and future outlook. *Current Opinion in Psychology*, *29*, 229–238.

Vieluf, S., Mora, K., Gölz, C., Reuter, E. M., Godde, B., Dellnitz, M., et al. (2018). Age- and expertise-related differences of sensorimotor network dynamics during force control. *Neuroscience*, *388*, 203–213.

Voelcker-Rehage, C., Reuter, E.-M., Vieluf, S., & Godde, B. (2013). Influence of age and expertise on manual dexterity in the work context. In C. M. Schlick, E. Frieling, & J. Wegge (Eds.), *The Bremen-hand-study@jacobs BT - age-differentiated work systems* (pp. 391–415). Berlin, Heidelberg: Springer Berlin Heidelberg.

Ward, N. S., & Frackowiak, R. S. J. (2003). Age-related changes in the neural correlates of motor performance. *Brain : A Journal of Neurology*, *126*, 873–888.

Yordanova, J., Falkenstein, M., & Kolev, V. (2020). Aging-related changes in motor response-related theta activity. *International Journal of Psychophysiology*, *153*, 95–106.

Zich, C., Debener, S., De Vos, M., Frerichs, S., Maurer, S., & Kranczioch, C. (2015). Lateralization patterns of covert but not overt movements change with age: An EEG neurofeedback study. *NeuroImage*, *116*, 80–91.